A COMPARISON OF INTERNAL AND EXTERNAL TURBULENT BOUNDARY LAYERS

Nick Hutchins, Jason Monty, Min Chong & Ivan Marusic
Walter Bassett Aerodynamics Laboratory, Mechanical and Manufacturing Engineering, University of Melbourne, Victoria 3010 Australia.

Summary This paper details a preliminary comparison between streamwise velocity fluctuations in turbulent channel flow and in zero-pressure-gradient flat-plate turbulent boundary layers. The unique facilities available at the University of Melbourne enable us to obtain these two flows at matched friction Reynolds numbers Re_τ and matched viscous-scaled hot-wire lengths l^+. We believe that this is the first time that such a precise and direct comparison has been made between internal and external wall-bounded turbulent flows. Detailed maps of energy spectra reveal important differences between these two flows, particularly in the very large-scale structures that exist in the log and inner wake regions. In the near future we plan to also obtain similar data for a fully turbulent pipe flow.

INTRODUCTION

Despite obvious differences in the wake regions of the mean velocity profiles, there has been a generally held belief, in the past at least, that wall-bounded turbulence in internal and external geometries behave very similarly in the viscous regions and that to some extent this similarity extends to the overlap (logaithmic) region. The apparent similarities for both geometries between inner-scaled mean velocity and turbulence intensity profiles would have leant some weight to this view, as would the observed similarity of the near-wall cycle between channel and boundary layer flows. More recently, the advent of Particle Image Velocimetry (PIV) as an experimental tool, along with the increasing availability of higher Reynolds number data sets, both experimental and numerical, has afforded a much clearer view of the log region. One consequence of this work has been a growing evidence that certain dominant length-scales might be different for pipes and channels than for boundary layers. Early indications of these differences came from measurements of cross correlation coefficients and energy spectra of streamwise velocity fluctuations in the streamwise and spanwise directions. Through analysis of premultiplied spectra ($k_x\phi_{uu}$, where k_x is the streamwise wavenumber, and ϕ_{uu} is the energy spectrum of streamwise velocity fluctuations), Kim & Adrian [5] have reported lengthscales of up to 14 radii in pipe flows. This is in contrast to peak length-scales of 6δ found from similar measurements in the log region of boundary layers [2]. By comparing the log region peak in $k_y\phi_{uu}$ (where k_y is the spanwise wavenumber) between channel DNS and boundary layer experiments [7, 1, 4], Hutchins & Marusic [3] have noted that the width of the large-scale structures in internal geometries are larger than those in boundary layers (by a factor of approximately 1.6). Monty *et al.* [6] have proven definitively this tendency through an in-depth analysis of experimental channel and pipe correlations.

FACILITY

The channel has a working section of approximately $22 \times 1.17 \times 0.1(2h)$ m. Measurements are made $175(2h)$ downstream of the tripped inlet to the working section. The working Reynolds number range for this facility is $1000 \lesssim Re_\tau \lesssim 4000$. The High Reynolds Number Boundary Layer Wind Tunnel (HRNBLWT) is an open-return blower wind-tunnel with working section $27 \times 2 \times 1$ m. The nominal Reynolds number range for this facility is $1000 \lesssim Re_\tau \lesssim 25\,000$. A matched target Kármán number of $Re_\tau \approx 4000$ was selected for comparison. All measurements were made using single-normal wire hot-wire probes with sensor length l and diameter d.

		flow				hot-wire details					acquisition		
facility	Re_τ	x (m)	U_∞ ms^{-1}	δ (m)	ν/U_τ (μm)	l (mm)	d (μm)	l/d	l^+	Δt_s^+	f_s (kHz)	f_{lp} (kHz)	$\left(\frac{TU_\infty}{\delta}\right)$
channel	3917	17.5	31.51	0.050	12.7	0.36	2.5	200	28	0.95	100	50	75 600
boundary layer	3843	5.2	17.2	0.096	25	0.75	3.75	200	30	0.41	60	30	16 200

The above table gives full details of the matched experiments. f_s and f_{lp} show sampling frequency and low-pass filter settings, Δt^+ gives the inner-scaled sample interval, and $\frac{TU_\infty}{\delta}$ shows the sample length as boundary layer turn-over times.

RESULTS

Figure 1(a) shows the inner-scaled mean turbulence intensities for both geometries. Within a $\pm 2\%$ error band, which ought to be considered an approximate confidence level (due to errors in hot-wire measurements, determination of U_τ etc) both profiles show remarkable similarity. However, a scale-by-scale analysis of the energy composition reveals some fundamental differences between the two flows, that are not discernable from the broadband intensities. Figure 1(b) shows an energy map of pre-multiplied streamwise energy spectra for all wall normal positions across the shear layers. The construction of these plots is introduced in some detail in [2, 3]. Such plots are useful since they show the magnitude of the fluctuating u energy (height of contours) at each wavelength (y-axis) and for each position z from the wall (x-axis).

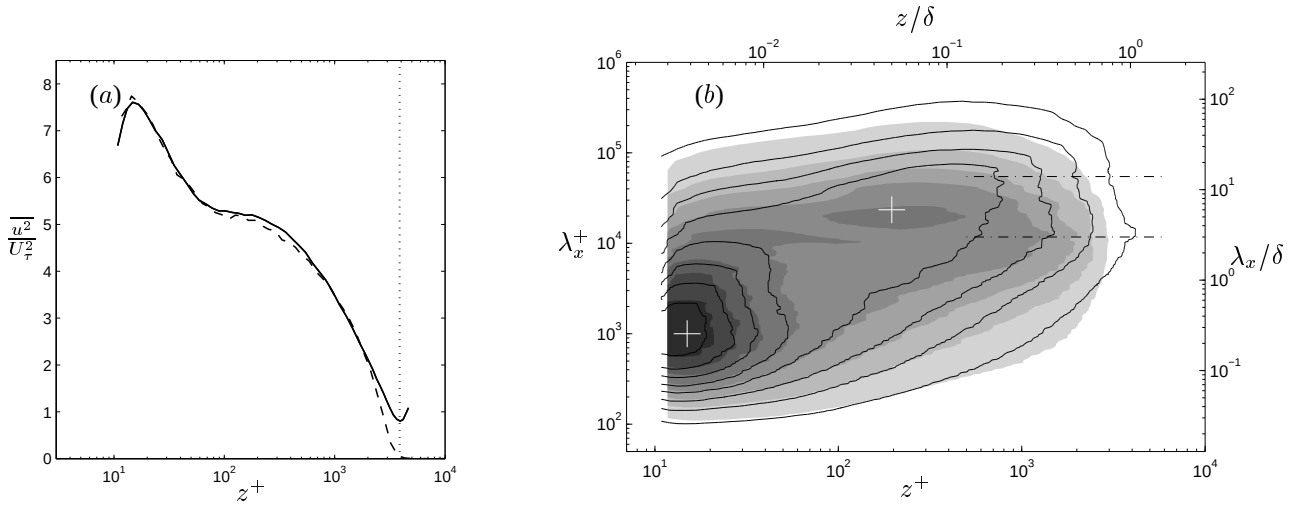

Figure 1. (a) mean intensities and (b) pre-multiplied spectra maps; (solid) channel; (dashed / shaded contours) boundary layer. Contours levels show $\frac{k_x\phi_{uu}}{U_\tau^2} = 0.2$ to 1.8 in increments of 0.2

The shaded contours show the pre-multiplied energy map for the boundary layer, with a shape and form very similar to that recorded previously [2, 3] exhibiting two pronounced peaks occurring at $z^+ \approx 15$, $\lambda_x^+ \approx 1000$ (the inner peak) and $z^+ \approx 0.05Re_\tau$, $\lambda_x^+ \approx 6Re_\tau$ (the outer peak). These two peaks are marked by the white $+$ symbols. The inner peak corresponds to the near-wall cycle, whilst the outer peak is believed to be due to very long meandering regions of elongated momentum deficit (termed 'superstructures' by [2]). Whilst the channel spectra map (shown by the unshaded contours) seems to follow that of the boundary layer close to the near wall peak, there is a marked deviation of the two sets of contours occurring in the log region of the flows (the log region is approximately located within $100 \lesssim z^+ \lesssim 600$). This deviation continues increasing into the wake. There is no sign of the outer peak for the channel. Instead the energy seems to organize into longer modes, close to approximately $14h$. Kim & Adrian [5] find that the energy in the log and core regions of pipe flows is contained in two peaks that they term Large-Scale Motion (LSM $\sim 3r$) and Very Large-Scale Motions (VLSM $\sim 14r$). The arrangements of energy in the channel seem to be somewhat similar. These two length-scales are marked by the horizonal chain-dashed lines on Figure 1(b). The fact that the energy is contained in different scales, and yet the total broadband intensity remains almost the same between geometries (up to $z^+ \approx 2000$), might suggest that the additional internal geometry constraint on turbulent channel flows somehow affects a *redistribution* of energy into larger scales. Figure 2 shows the difference in pre-multiplied energy between the channel and boundary layer (contours show $\Delta\frac{k_x\phi_{uu}}{U_\tau^2}$ from $^-0.2$ to 0.2 in 0.05 increments). Solid contours show regions of increased energy, whilst dashed contours show regions where the channel is less energetic than the boundary layer. Clearly the largest differences seem to be centered around $z^+ = 1000$ (in the wake region $z/\delta \approx 0.25$), with the channel exhibiting increased energy in scales larger than $\lambda_x \approx 9\delta$, and decreased energy in scales smaller than this (as compared to the boundary layer energy distribution). In summary, we have demonstrated obvious differences in energy distributions between channels and boundary layers. Although such differences are greatest in the wake region, it is shown that differences extend all the way through the log region and into the viscous buffer region.

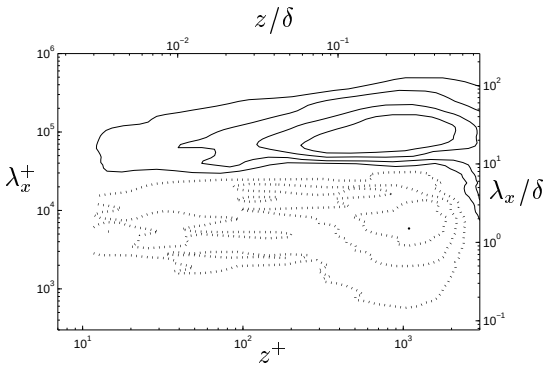

Figure 2. Difference in $\frac{k_x\phi_{uu}}{U_\tau^2}$ maps between geometries.

References

[1] H. Abe, H. Kawamura, and H. Choi. Very large-scale structures and their effects on the wall shear-stress fluctuations in a turbulent channel flow up to $Re_\tau = 640$. *J. Fluids Eng.*, 126:835–843, 2004.

[2] N. Hutchins and I. Marusic. Evidence of very long meandering features in the logarithmic region of turbulent boundary layers. *J. Fluid Mech.*, 579:1–28, 2007.

[3] N. Hutchins and I. Marusic. Large-scale influences in near-wall turbulence. *Phil. Trans. R. Soc. A*, 365:647–664, 2007.

[4] KN. Kasagi, K. Fukagata, and Y. Suzuki. Adaptive control of wall-turbulence for skin friction drag reduction and some consideration for high Reynolds number flows. In *2nd International Symposiumon Seawater Drag Reduction*, 2005. Busan.

[5] K. C. Kim and R. Adrian. Very large-scale motion in the outer layer. *Phys. Fluids*, 11:417–422, 1999.

[6] J. P. Monty, J. A. Stewart, R. C. Williams, and M. S. Chong. Large-scale features in turbulent pipe and channel flows. *J. Fluid Mech.*, 589, 2007. 147–156.

[7] C. D. Tomkins and R. J. Adrian. Spanwise structure and scale growth in turbulent boundary layers. *J. Fluid Mech.*, 490:37–74, 2003.